Numerical Study of Navier-Stokes Equations in Supersonic Flow over a Double Wedge Airfoil using Adaptive Grids

Ramesh Kolluru[1] and Vijay Gopal[1]
[1]BMS College of Engineering, Bangalore, Karnataka, India
*Corresponding author: BMS College of engineering, Bangalore 560 019, aero.g.vijay@gmail.com

Abstract: Numerical study of aerodynamic characteristics in steady laminar supersonic flow over a double wedge airfoil is carried out using finite element based CFD software tool "Comsol Multiphysics". The aerodynamic characteristics namely; lift and drag are analysed by numerically solving compressible Navier-Stokes equations in the flow field around double wedge airfoil by parameterising the angle of attack α and thickness to chord ratio $\frac{t}{c}$. The present work makes use of "high Mach number flow" module provided in Comsol Multiphysics with pseudo time stepping methodology and adaptive gridding technique to obtain a steady state solution by marching in time by capturing the shocks and expansions occurring in the flow field. The results obtained from the CFD tool are compared with inviscid shock expansion theory and are found to be in good agreement with the same.
Keywords: Pardiso, Angle of attack, supersonic airfoil, shock.

1. Introduction: The supersonic aerofoils are broadly classified into two types; biconvex aerofoil and double wedge aerofoil whose cross-sectional profiles are indicate in **Figure 1**.
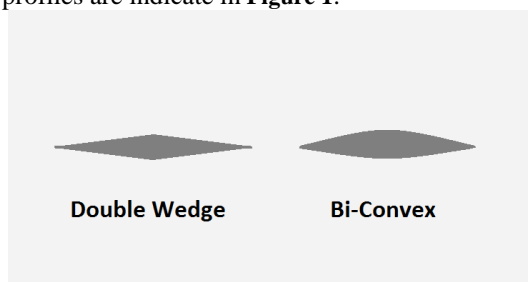
Figure 1: Cross-sectional view of typical supersonic aerofoil.

Existence of such bodies in the supersonic flow field creates singularities in the flow such as shock and expansion waves. The effect of these singularities when such aerofoils are used in supersonic flight increases the drag which is undesirable. This additional component of drag other than form and skin drag is often referred to as wave drag and it is found that this component of drag can be minimised if the shock is kept attached to the body in flight. This can be achieved by designing a thinner cross-section along with sharp leading and trailing edges unlike subsonic aerofoil whose rounded leading edge produces a detached shock [10] which causes greater drag compared to the attached shock. Therefore the profiles indicated in **Figure 1** are designed to have a better lift to drag ratio as compared to subsonic aerofoils in supersonic flight [4]. In the present work an attempt is made to study the aerodynamic response of 2D double wedge aerofoil in supersonic flow with free stream Mach number of 2.5 by varying the angle of attack and thickness to chord ratio by performing numerical simulation using adaptive grids. The results thus obtained from numerical solution are compared with shock-expansion theory results.

1.2. Aerodynamic coefficients: These are non-dimensional numbers which are independent of density and free stream velocity which enables us to generalise the important aerodynamic parameters such as lift and drag of the aerofoil [8]. In the following discussion we evaluate and analyse pressure (1) lift (2) and drag (3) coefficients for an aerofoil with chord length 'c' and span 1m.

$$C_p = \frac{p - p_\infty}{\frac{1}{2} \cdot \rho_\infty \cdot V_\infty^2} \qquad (1)$$

$$C_L = \frac{L}{\frac{1}{2} \cdot \rho_\infty \cdot V_\infty^2 \cdot c} \qquad (2)$$

$$C_D = \frac{D}{\frac{1}{2} \cdot \rho_\infty \cdot V_\infty^2 \cdot c} \qquad (3)$$

1.3 Geometry of aerofoil: The symmetrical double wedge aerofoil design are characterised by two salient geometrical parameters namely; maximum thickness (t_a) and chord length (c_a) as indicated in **Figure 2**.
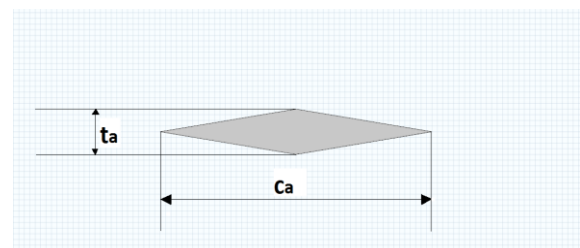
Figure 2: Schematic diagram indicates the geometry of double wedge aerofoil.

3. Governing equation of fluid: In the current study, laminar time dependent compressible Navier-Stokes equations are solved to obtain a steady state solution by marching in time. The compressible Navier-Stokes [6] consists of conservation laws of mass (4), momentum (5) and enthalpy (6). These equations are solved for a 2D flow field over a double wedge aerofoil. The FEM tool uses a non-conservative form of the governing equations as described below

$$\frac{\partial \rho}{\partial t} + \rho \cdot \nabla \cdot (\boldsymbol{u}) + (\boldsymbol{u} \cdot \nabla)\rho = 0 \tag{4}$$

$$\rho\left(\frac{\partial \boldsymbol{u}}{\partial t} + (\boldsymbol{u} \cdot \nabla)\boldsymbol{u}\right) = \nabla \cdot \left[-p \cdot \boldsymbol{I} + \mu \cdot \left((\nabla \boldsymbol{u}) + (\nabla \boldsymbol{u})^T - \frac{2}{3} \cdot \nabla \cdot \boldsymbol{u} \cdot \boldsymbol{I}\right)\right] \tag{5}$$

$$\rho \cdot C_p\left(\frac{\partial T}{\partial t} + (\boldsymbol{u} \cdot \nabla)T\right) = \nabla \cdot (k \cdot \nabla T) + \frac{T}{\rho} \cdot \left(\frac{\partial \rho}{\partial T}\right)_p\left(\frac{\partial p}{\partial t} + (\boldsymbol{u} \cdot \nabla)p\right) +$$

$$\nabla \boldsymbol{u} : \left(\mu \cdot \left((\nabla \boldsymbol{u}) + (\nabla \boldsymbol{u})^T - \frac{2}{3} \cdot \nabla \cdot \boldsymbol{u} \cdot \boldsymbol{I}\right)\right) \tag{6}$$

To obtain closed form equations, the thermo-dynamic state relation for ideal gas is used .The viscosity variation with temperature is solved using the help of Sutherland's law described in expression (7) while the thermal conductivity k is directly obtained from the material library in FEM tool.

$$\mu = \mu_{ref}\left(\frac{T}{T_{ref}}\right)^{\frac{3}{2}}\left(\frac{T_{ref} + S}{T + S}\right) \tag{5}$$

Where T_{ref}=273K, μ_{ref}=1.716e-5Pa-s, S=111K.

5. Simulation model: The model is constructed in the GUI provided in Comsol Multi-physics for a 2D case as depicted in **Figure 3**.
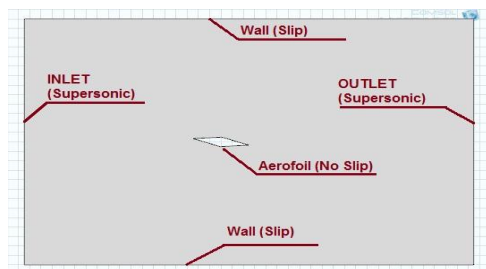
Figure 3: 2D Simulation model in Comsol where the shaded region depicts the flow regime.

The model contains an inlet and an outlet with two slip walls above and below the aerofoil which is placed in the centre. The flow is numerically simulated for aerofoil having thickness to chord ratio ($t_c = \frac{t}{c}$) of 0.08, 0.1 and 0.12. The chord length is 1m for all the cases while only the thickness is varied. For each case of t_c the angle of attack (α) in anti-clockwise direction is varied from the values in the set given by; (0^0, 1^0, 2^0, 3^0, 4^0, 5^0, 8^0 and 12^0). The dimensions of the boundaries are chosen such that the shock reflections from the walls are kept at minimum level.

6. Boundary and initial Conditions: The free stream conditions that will be considered in this study will be similar to the atmosphere conditions that prevail at 12km altitude [9]. The boundary and initial conditions are given by:
a) Wall: Slip condition.
b) Aerofoil: No slip condition.
c) Inlet: M=2.5, T=218K and p=0.2atm.
d) Outlet: $\nabla T = 0$.
The initial conditions specified for the domain are:
a) Domain variables: p=0.2atm, T=218K
b) Domain Velocity: u_x= 600m/s, u_y= 0m/s.

7. Grid and Solver: Comsol Multi-physics provides a wide variety of meshing and solver options. As the flow is characterised by shock wave, consequently high gradients of primary variables exist, to capture this, adaptive meshing on unstructured triangular mesh is implemented as depicted in **Figure 4**. Also the boundary layer effect [7] is captured by using 6 to 8 rectangular cell grids on boundaries having no-slip condition. The boundary layer mesh thickness and growth rate is varied accordingly for each case for desired result. The type of mesh interpolation or element order is selected in Comsol Multi-physics to be "P1+P1" which indicates first order element type for velocity and pressure which is used for FEM computation.
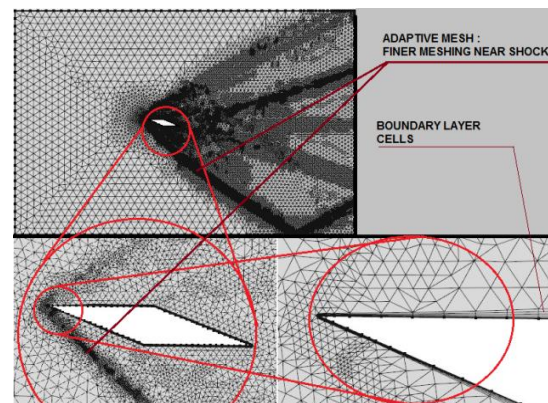

Figure 4: Adaptive grid for t_c=0.1 and α=12^0case.

To solve for a particular case, the Euler equations are solved first whose solution is made the initial condition for obtaining viscous solution. All the primary variables in the solver are fully coupled using pseudo time stepping with a stationary solver. The stationary solver uses PARDISO (Parallel Sparse Direct Linear Solver) [3] which is capable of solving large sparse symmetric and unsymmetrical linear system of equations with good memory efficiency along with nested dissection multithreaded pre-ordering algorithm. For all the cases the tolerance was made 0.01 which was convergence the criteria for numerical simulation. To any curb convergence problem the CFL number was made 0.9 for few cases.

2

8. Results and analysis: The aerodynamic coefficients are evaluated using both shock-expansion (SE) theory and numerical simulation of Navier-Stokes (NS). To solve the flow through shock-expansion theory [2], [5] for various geometries and angle of attack, a MATLAB code was developed **Appendix-I**. This code makes use of oblique shock relations and Prandtl-Meyer relation along with required thermodynamics to evaluate the aerodynamic coefficients for the current study. For the numerical simulations, y-axis was made perpendicular to free stream direction while x-axis was along it. The lift and drag per unit span was obtained by line integration of total stress along the airfoil in y and x direction respectively. Thus the coefficient of lift (C_L) and drag (C_D) are evaluated for all cases of t_c and α, where the values of α are (0^0, 1^0, 2^0, 3^0, 4^0, 5^0, 8^0 and 12^0) and that of t_c are (0.08, 0.10 and 0.12). The C_L v/s α graph which is obtained from SE theory is plotted in **Figure 5** while that obtained from numerical simulation of Navier-Stokes equations is plotted in **Figure 6**.
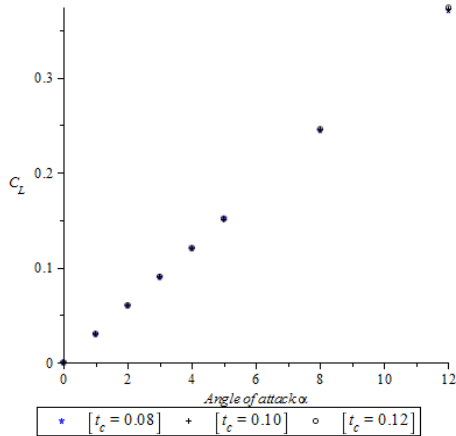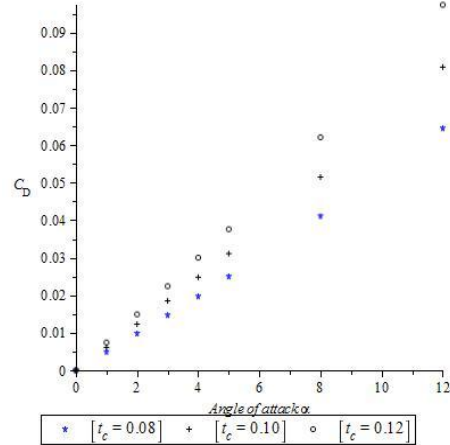

Figure 5: Graph indicates the variation of C_L with α which is obtained from shock-expansion theory for t_c = (0.08, 0.10 and 0.12).
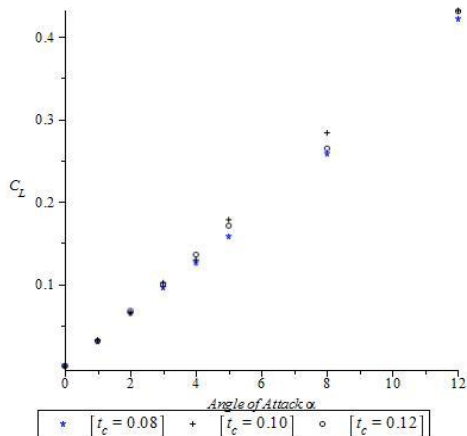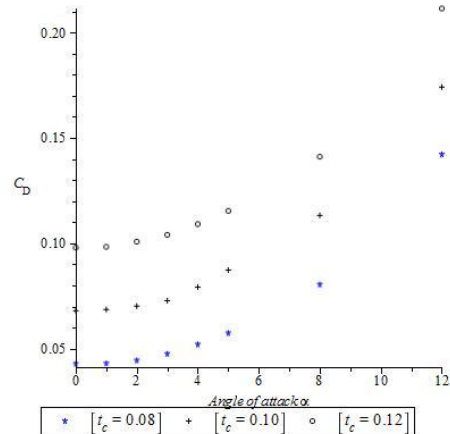

Figure 6: Graph indicates the variation of C_L with α which is obtained from solving Navier-Stokes for t_c = (0.08, 0.10 and 0.12).

Although the behaviour of C_L with t_c cannot be generalised, its variation is proportional to angle of attack and found to be linear, also close observation reveal that the SE theory is less sensitive to variation of t_c while significant variation is captured in Navier-Stoke solution. The plot of C_D v/s α for both for both SE theory **Figure 7** and Navier-Stoke solution **Figure 8** are plotted.


Figure 7: Graph indicates the variation of C_D with α which is obtained from shock-expansion theory for t_c = (0.08, 0.10 and 0.12).


Figure 8: Graph indicates the variation of C_D with α which is obtained from solving Navier-Stokes for t_c = (0.08, 0.10 and 0.12).

From the plots represented in **Figure7**, **8**, the behaviour of C_D with α for SE theory is observed to be linear while that for numerical simulation of NS equations is non-linear, also, it can be seen that C_D increases with t_c irrespective of SE or NS solutions. The contribution to drag in a supersonic flight is mostly from wave drag. The SE theory only captures this wave-drag while the numerical simulation of NS equations captures wave, form and skin drag which substantiates the observation from plot that for a particular value of α, the value of C_D in case of NS solutions is higher when compared to the values obtained from SE theory. To explore this observation more closely, the relative percentage error between NS and SE solutions with respect to NS solutions for C_L and C_D values for a specific case t_c=0.1 v/s α are plotted in **Figure 9, 10** respectively.

3
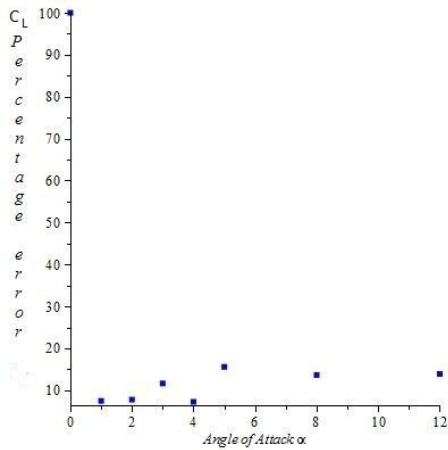
Figure 9: Plot for relative percentage error between the values of C_L obtained from NS and SE solutions with respect to NS solution v/s α for $t_c = 0.10$.
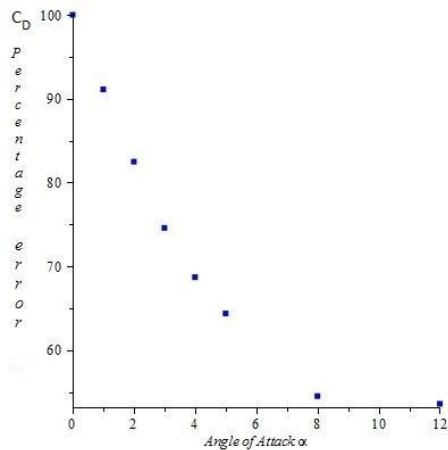

Figure 10: Plot for relative percentage error between the values of C_D obtained from NS and SE solutions with respect to NS solution v/s α for $t_c = 0.10$.

8.1 Result and analysis of specific cases: To obtain a detailed insight into the numerical solution, two cases are inspected for aerofoil designed with t_c =0.10. For the first case α = 4^0 while for second it is 12^0. The aerodynamic coefficient C_p as defined in Section **1.2** indicates the variation in pressure along the aerofoil for both top and bottom surface which is plotted for α=4^0 and 12^0 as indicated in **Figure 11, 12**.
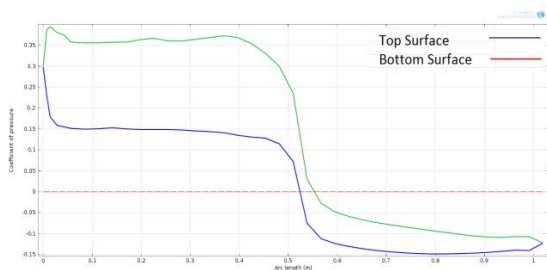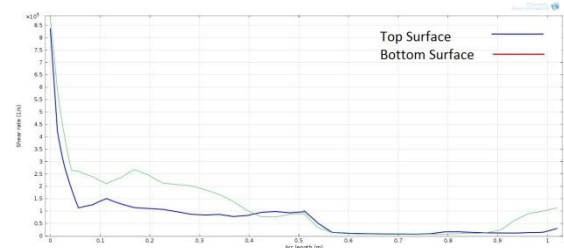

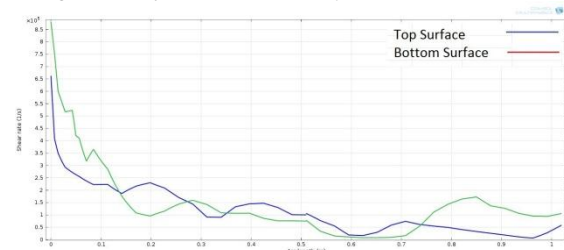**Figure 11:** Graph plotted for C_p v/s Arc length long the boundary of aerofoil with t_c=0.10 and α=4^0.
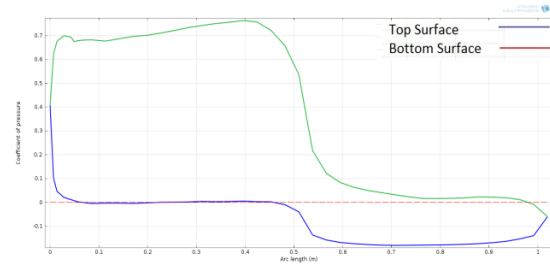
Figure 12: Graph plotted for C_p v/s Arc length of along boundary of aerofoil with t_c=0.10 and α=12^0.

From the graph plotted in **Figure 11, 12** it can be observed that the values of C_p in the fore region of airfoil increases with positive angle of attack at the bottom surface as the shock strengthens while that for top surface the shock weakens eventually causing expansion at higher angle of attack. Therefore from the above argument it can be concluded that in the fore region of the airfoil the amount difference in C_p between top and bottom surface increases with angle of attack, also, argument based on similar lines can substantiate the increase in difference in C_p between top and bottom surface in the aft part of aerofoil. As the inferences regarding viscous effect cannot be drawn from C_p, the shear rate provides insight into the same which is plotted for both top and bottom surface of aerofoil at α = 4^0 and 12^0 in **Figure 13** and **Figure 14** respectively.


Figure 13: Graph plotted for Shear rate v/s Arc length along boundary of aerofoil with t_c=0.10 and α=4^0.
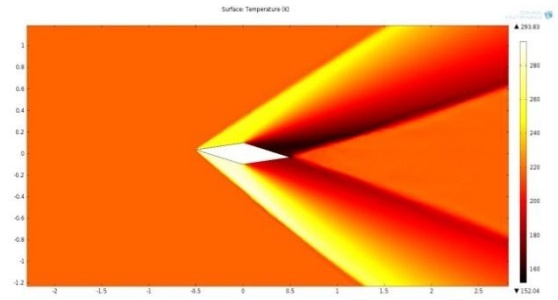

Figure 14: Graph plotted for Shear rate v/s Arc length along boundary of aerofoil with t_c=0.10 and α=12^0.

It is evident from the plots above that a stronger shock region is subjected to a higher shear rate which increases the wall shear stress as compared to a weaker shock region. The effect of increasing the angle of attack increases the strength of the shock region in lower surface and weakens it at upper surface. This can be better visualised by surface plots of pressure **Figure 15, 16**, Mach number **Figure 17, 18** and temperature **Figure 19, 20** and density contours **Figure 21, 22**.
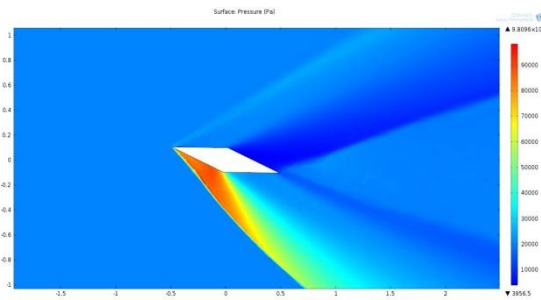
4
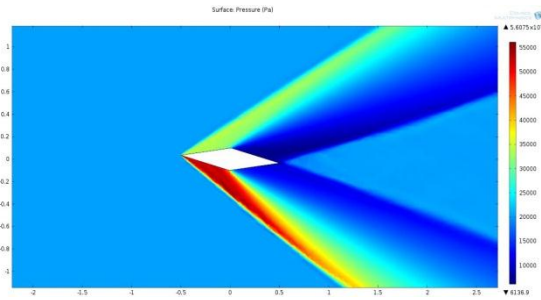
Figure 15: Surface plot of pressure for t_c=0.10 and α=4^0.

Figure 16: Surface plot of pressure for t_c=0.10 and α=12^0.

Figure 17: Surface plot of Mach number for t_c=0.10 and α=4^0 with two stream lines.

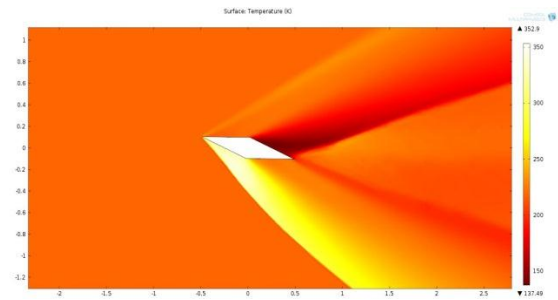**Figure 18:** Surface Plot of Mach number for t_c=0.10 and α=12^0 with two stream lines.
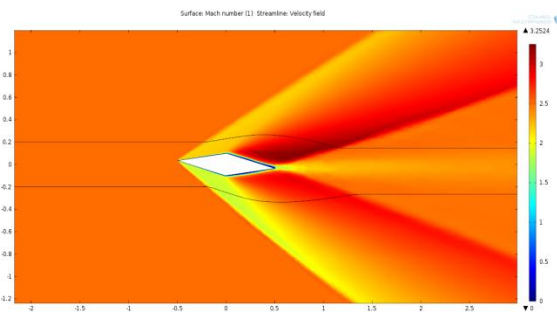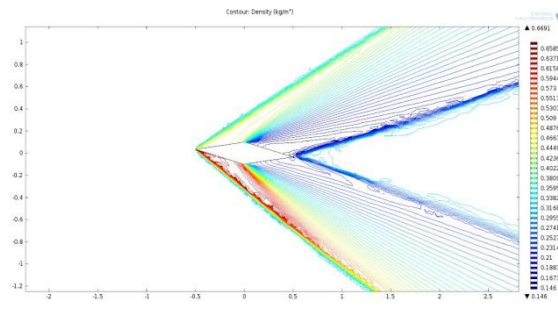

Figure 19: Surface plot of temperature for t_c=0.10 and α=4^0.

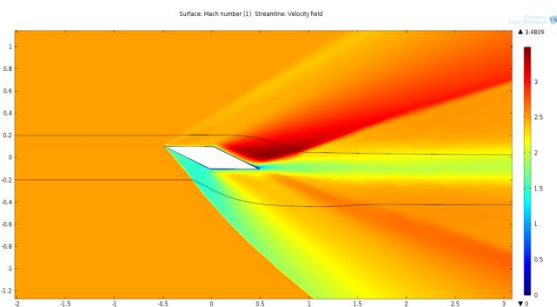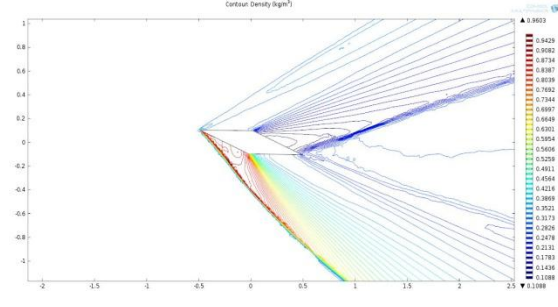**Figure 20:** Surface plot of temperature for t_c=0.10 and α=12^0.

Figure 21: Density contour plot for t_c=0.10 and α=4^0.

Figure 22: Density contour plot for t_c=0.10 and α=4^0.

5

9. Conclusion: The solution obtained from numerical simulation performed with FEM tool is in good agreement with shock-expansion theory indicating the fundamental flow field behaviour to be same. The difference in the values of coefficients obtained from SE-theory and compressible NS numerical simulation indicates the expected viscous and wake effects that exist in nature. Thus Comsol Multiphysics simulates the flow to acceptable standards providing the users a platform to simulate high Mach number flow along with other required physics. The double wedge aerofoil was simulated for 24 cases with inlet conditions similar to atmospheric conditions that prevail at 12km cruise altitude and with free stream Mach number M=2.5. The values of coefficients thus obtained from numerical simulation in the current study are only applicable for infinite span wing having airfoil section congruent to aerofoil designed in this current work [1]. In the range of parameters that are varied in this study no flow separation was observed on the aerofoil surface in any of the cases. The MATLAB code **Appendix-I** which was developed in the current study implements SE theory to evaluate aerodynamic coefficients for double wedge airfoil is capable of computing attached shock cases only and not otherwise.

References:

[1]. D.Beastall, R.J.Pallant, Wind-tunnel test on two-dimensional aerofoils at M=1.86 and M=2.48, Aeronautical research council reports and memoranda, National Aeronautical establishment.

[2]. John D Anderson, Modern compressible flow, third edition, Mc Graw hill.

[3]. Frank E. Curtis, Johannes Huber, Olaf Schenk, Andreas Wachter, On the Implementation of an Interior-Point Algorithm for Nonlinear Optimization with Inexact Step Computations.

[4]. Stephen M.Ruffin, Anurag Gupta, David Marshall, Supersonic Channel Aerofoils for Reduced Drag, AIAA journal Vol.38,No.3, March 2000.

[5]. Dean R, Chapman, Airfoil profiles for minimum pressure drag at supersonic velocities-application of shock-expansion theory including consideration of hypersonic range, NACA technical note 2787.

[6]. Benoit Desjardins, Chi-Kun Lin, A survey of the Compressible Navier-Stokes equations, TAIWANESE Journal of Mathematics, Vol 3, No2,pp. 123-137, June 1999.

[7]. W.P. Graebel, Advanced Fluid Mechanics, Academic Press ELSEVIER.

[8]. John D Anderson, Introduction to flight, fifth edition, Mc Graw hill.

[9]. Raymond L. Barger, Some effects of flight path and atmospheric variations on boom propagation from supersonic aircraft, NASA technical report r-191.

[10]. Reza Nilifard, Hossein Ahmadikia, Supersonic flow over blunt body using direct simulation Monte Carlo method and Navier-Stokes equation, Adv.Theor.Appl.Mech.,Vol.3, 2010, no.2,75-87.

Appendix-I

```matlab
clear all;
close all;
clc;
disp('LIFT,DRAG,PRESSURE,TEMPERATURE,Cl and CD EVALUATION FOR DOUBLE WEDGE AEROFOIL FOR')
disp('ATTACHED SUPERSONIC FLOW ')
disp('.')
disp('.')
disp('ENTER THE FOLLOWING DATA WITH FREE STREAM DIRECTED TO RIGHT SIDE')
t=input('enter the value of maximum thickness of doublewedge aerofoil in meters   ');
c=input('enter the value of chord length of doublewedge aerofoil in meters   ');
M=input('enter the free stream Mach number  ');
degrees=input('enter the anti-clockwise angle of attack in degrees   ');
P=input('enter the free stream static pressure in pascals   ');
r=input('enter the ratio of specific heats   ');
R=input('enter specific gas constant in [J/(Kg.K)]   ');
T=input('enter free stream Temperature in kelvin   ');
a=abs(degrees./57.2957795);
e=atan(t./c);
cs=sqrt(r.*R.*T);
l=0.5.*(sqrt(t.^2+c.^2));
Dv=((M.^2-1).^2-3.*(1+((r-1)./2).*(M.^2)).*(1+((r+1)./2).*(M.^2)).*((tan(abs(e)+abs(a)).^2)));
if(Dv<0)
    disp('.')
    disp('.')
disp('detached shock exist or invalid data entry: Computation not possible !');

else
    SWDv=input('enter 1 for weak shock case or 0 for strong shock case ');
    if(SWDv==1|SWDv==0)
        Q2=abs(e)-abs(a);
        disp('.')
        disp('.')
        disp('.')
        disp('SOLUTION')
        disp('>Valid data entered for free stream condition')
        if(Q2>0)

        disp('>Fore upper region of aerofoil under goes a shock wave')
        lambda=((M.^2-1).^2-3.*(1+((r-1)./2).*(M.^2)).*(1+((r+1)./2).*(M.^2)).*((tan(Q2).^2)).^(1./2);
        chi=((M.^2-1)^3-9.*(1+((r-1)./2).*(M.^2)).*(1+((r-1)./2).*(M.^2)+((r+1)./4).*(M.^4)).*(tan(Q2).^2)./((lambda).^3;
        B2=atan((M.^2+2.*(lambda).*cos((4*pi*SWDv+acos(chi)./3))./(3.*(1+((r-1)./2).*(M.^2)).*tan(Q2));
        P2=P.*(1+((2.*r)./(r+1)).*((M.*sin(B2)).^2-1));
        M2=(sqrt(((M.*sin(B2).^2)+(2./(r-1)))./(((2.*r)./(r-1)).*M.*sin(B2)-1)))./(sin(B2-Q2));
        T2=T.*(1+((2.*r)./(r+1)).*((M.*sin(B2)).^2-1)).*(((r-1).*(M.*sin(B2).^2)+2)./((r+1).*(M.*sin(B2).^2)));

        else
        disp('>Fore upper region of aerofoil under goes a expansion')
        syms IM
        IM2=solve(abs(Q2)+sqrt((r+1)./(r-1)).*(atan(sqrt(((r-1)./(r+1)).*(M.^2-1))))-atan(sqrt(M.^2-1))-sqrt((r+1)./(r-1)).*(atan(sqrt(((r-1)./(r+1)).*(IM.^2-1))))+atan(sqrt(IM.^2-1)));
        M2=abs(IM2);
        P2=P.*((1+((r-1)./2).*(M.^2))./(1+((r-1)./2).*(M2.^2))).^(r./(r-1));
        T2=T.*((1+((r-1)./2).*(M.^2))./(1+((r-1)./2).*(M2.^2)));

        end
        disp('>Fore lower region of airfoil under goes a shock wave')
        Q3=abs(e)+abs(a);
        lambda1=((M.^2-1).^2-3.*(1+((r-1)./2).*(M.^2)).*(1+((r+1)./2).*(M.^2)).*((tan(Q3).^2)).^(1./2);
        chi1=((M.^2-1)^3-9.*(1+((r-1)./2).*(M.^2)).*(1+((r-1)./2).*(M.^2)+((r+1)./4).*(M.^4)).*(tan(Q3).^2)./((lambda1).^3;
        B3=atan((M.^2+2.*(lambda1).*cos((4*pi*SWDv+acos(chi1)./3))./(3.*(1+((r-1)./2).*(M.^2)).*tan(Q3));
        P3=P.*(1+((2.*r)./(r+1)).*((M.*sin(B3)).^2-1));
        M3=(sqrt(((M.*sin(B3).^2)+(2./(r-1)))./(((2.*r)./(r-1)).*M.*sin(B3)-1)))./(sin(B3-Q3));
        T3=T.*(1+((2.*r)./(r+1)).*((M.*sin(B3)).^2-1)).*(((r-1).*(M.*sin(B3).^2)+2)./((r+1).*(M.*sin(B3).^2)));

        disp('>Aft upper region of aerofoil under goes expansion')
        Q4=2.*abs(e);
        syms IMA
        IM4=solve(Q4+sqrt((r+1)./(r-1)).*(atan(sqrt(((r-1)./(r+1)).*(M2.^2-1))))-atan(sqrt(M2.^2-1))-sqrt((r+1)./(r-1)).*(atan(sqrt(((r-1)./(r+1)).*(IMA.^2-1))))+atan(sqrt(IMA.^2-1)));
        M4=abs(IM4);
        P4=P2.*((1+((r-1)./2).*(M2.^2))./(1+((r-1)./2).*(M4.^2))).^(r./(r-1));
        T4=T2.*((1+((r-1)./2).*(M2.^2))./(1+((r-1)./2).*(M4.^2)));

        disp('>Aft lower region of aerofoil under goes expansion')
        Q5=2.*abs(e);
        syms IMB
        IM5=solve(Q5+sqrt((r+1)./(r-1)).*(atan(sqrt(((r-1)./(r+1)).*(M3.^2-1))))-atan(sqrt(M3.^2-1))-sqrt((r+1)./(r-1)).*(atan(sqrt(((r-1)./(r+1)).*(IMB.^2-1))))+atan(sqrt(IMB.^2-1)));
        M5=abs(IM5);
        P5=P3.*((1+((r-1)./2).*(M3.^2))./(1+((r-1)./2).*(M5.^2))).^(r./(r-1));
        T5=T3.*((1+((r-1)./2).*(M3.^2))./(1+((r-1)./2).*(M5.^2)));
        else
            disp('.')
            disp('.')
            disp('.')
            disp('invalid information')
        end

end

L=l.*((P5-P2).*cos(abs(e)-abs(a))+(P3-P4).*cos(abs(e)+abs(a)));
D=l.*((P5-P2).*sin(abs(e)-abs(a))+(P3-P4).*sin(abs(e)+abs(a)));
RLD=L./D;
V=M.*cs;
dp=(0.5).*((P)./(R.*T)).*(V.^2);
CL=(L)./(dp.*c);
CD=(D)./(dp.*c);
ch=-c./10:c./10:c;
fore=[ones(1,5),zeros(1,5)];
aft=[zeros(1,5),ones(1,5)];
disp('.')
disp('Lift per unit span length L(N/m) is :')
eval(L)
disp('Drag per unit span length D(N/m) is :')
eval(D)
disp('Lift to Drag ratio is :')
eval(RLD)
disp('Coefficient of lift is')
eval(CL)
disp('Coefficient of drag is')
eval(CD)
disp('FIGURE 1 :Coefficient of pressure CP plot on the surface of aerofoil ')
CP_u=((P2-P).*fore+(P4-P).*aft)./dp;
CP_l=((P3-P).*fore+(P5-P).*aft)./dp;
figure(1)
plot(ch,CP_u,ch,CP_l),ylabel('CP'),xlabel('Chord Length'),legend('upper surface','lower surface');
disp('FIGURE 2 :Mach number plot on the surface of aerofoil ')
M_u=M2.*fore+M4.*aft;
M_l=M3.*fore+M5.*aft;
figure(2)
plot(ch,M_u,ch,M_l),ylabel('Mach number'),xlabel('Chord Length'),legend('upper surface','lower surface');
disp('FIGURE 3 :Pressure plot on the surface of aerofoil ')
P_u=P2.*fore+P4.*aft;
P_l=P3.*fore+P5.*aft;
figure(3)
plot(ch,P_u,ch,P_l),ylabel('Pressure in pascal'),xlabel('Chord Length'),legend('upper surface','lower surface');
disp('FIGURE 4 :Temperature plot on the surface of aerofoil ')
T_u=T2.*fore+T4.*aft;
T_l=T3.*fore+T5.*aft;
figure(4)
plot(ch,T_u,ch,T_l),ylabel('Temperature in Kelvin'),xlabel('Chord Length'),legend('upper surface','lower surface');
```